Load-Sharing Model for Polymer Cylindrical Gears

E. Letzelter, J.P. de Vaujany and M. Guingand

(First presented at the VDI International Conference on Gears, October 2010, Technical University of Munich)

Management Summary

This paper presents an original method to compute the loaded mechanical behavior of polymer gears. Polymer gears can be used without lubricant, have quieter mesh, are more resistant to corrosion, and are lighter in weight. Therefore their application fields are continually increasing. Nevertheless, the mechanical behavior of polymer materials is very complex because it depends on time, history of displacement and temperature. In addition, for several polymers, humidity is another factor to be taken into account. The particular case of polyamide 6.6 is studied in this paper.

The model to compute the viscoelastic displacement of the polymer materials is presented first. Numerous rheological models exist, but in this study the generalized Kelvin model has been chosen (*Ed.'s Note: Baron (Sir William Thomson) Kelvin (1824–1907), influential Scottish engineer, mathematician and physicist.*)

This model accounts for a wide relaxation time spectrum and—with the time temperature superposition principle—it is linked to temperature and humidity. In addition, a spectrometer experiment is conducted to characterize the mechanical properties at different temperature and humidity.

In a second part of this paper, the viscoelastic model is integrated in a quasi-static load-sharing computation developed by LaMCoS (Laboratory of Contact Mechanics and Structures, University of Lyon, Lyon, France). In calculus, the displacement is obtained with the displacement compatibility relation in a large meshing over the entire surface of the tooth. This relation integrates the viscoelastic displacement and the geometrical influence coefficients. These coefficients permit integration of the bulk and contact deformations. The method shown in this paper provides results such as the loaded transmission error; instantaneous meshing stiffness and pressure; load-sharing and the root tooth stresses at different temperature; and humidity and rotation speed.

Also, a test bench has been developed to measure the transmission error and the thermal behavior. This bench is presented in this paper.

Introduction

LaMCoS has developed numerical models to predict two essential areas—load-sharing and transmission error; they are needed in order to carry out dynamic studies. But these models have been developed for different gear geometries—made with elastic materials—as cylindrical gears (Ref. 1), face gears (Ref. 2), spiral bevel gears (Ref. 3), worm gears (Ref. 4) and pinion rack (Ref. 5). To determine the load-sharing, LaMCoS provides a solution for the displacement compatibility equation. The influence coefficients method is used to separate the contact and volume effects; this method has the advantage of being much less time consuming.

As mentioned, polymer gears present many advantages over steel gears: no lubricant; quieter mesh; and less weight. Generally, the polymer material chosen to produce molded or cut gears is a semi-crystalline polymer; i.e., polyamide (Ref. 6). The mechanical behavior of this polymer is viscoelastic and thus depends on the time, speed and history of displacement and temperature (Ref. 7). In addition, in the case of polyamide, the mechanical behavior depends also on humidity levels (Ref. 8).

Recently, Hiltcher et al. (Ref. 4) have developed a quasi-static load-sharing model of a metal worm gear with a polymer wheel. With this method, they assume that the displacement of the steel worm is negligible compared to that of the polymer wheel. But in this paper the method presented is adapted for polyamide 6.6 gears; therefore, the displacement of the polymer gear is addressed. In addition, the characterization of the mechanical properties is updated. This study is limited to the linear domain of the material and the assumption is made that the tooth is relaxed for each rotation.

Also, the original test bench developed by LaMCoS can measure the transmission error and thermal behavior of polyamide 6.6 gears. The transmission error simulated with the load-sharing model will be compared to the measured one; the thermal measurement is made with an infrared camera, which provides the evolution and repartition of the meshing temperature.

Mechanical Behavior of Polyamide 6.6

The mechanical behavior of polyamide is viscoelastic, meaning that it depends on loading duration or, in other words, on the history of displacement and temperature. Humidity is another factor to be taken into account in the specific case of polyamide 6.6.

The linear viscoelastic properties of polymers, i.e., the material temporal compliance $J(t)$, can be deduced from creep tests and simulated by a rheological model that introduces retardation times τ and the amplitude of the deformation. In the case of a unique retardation time, the temporal compliance can be expressed with the relation (Ref. 9):

$$J\left(t\right) = J_r \left(1 - \exp\left(\frac{-t}{\tau}\right)\right) \text{ with } \tau = \eta J_r \qquad (1)$$

J_r is the relaxed compliance and η is the viscosity.

Another technique to deduce viscoelastic properties is the spectrometer test. A DMA (dynamic mechanical analysis) was performed in torsion mode; the complex compliance $J^*(i\omega, T)$ or the complex elastic modulus $G^*(i\omega, T)$ can be deduced from the spectrometer test (Ref. 9):

$$J^*\left(i\omega, T\right) = \frac{1}{G^*\left(i\omega, T\right)} = J'(\omega, T) - iJ''(\omega, T) \qquad (2)$$

J' is the elastic compliance and J'' is the viscous one.

In order to simulate the viscoelastic behavior, the relationship in Equation 1 has a unique retardation time and is insufficient to account for the viscoelasticity of polyamide 6.6. Thus, a rheological model such as the generalized Kelvin model is proposed in order to account for a wide relaxation time spectrum (Ref. 9); this rheological model is presented in Figure 1.

In order to compute the load-sharing, knowledge of the temporal displacement of polyamide 6.6 material is necessary. Thus, the total strain of the generalized Kelvin model is computed in Equation 4. This requires use of an incremental scheme based on differential equations and the relationship can be written in each block of the model:

$$\sigma\left(t\right) = \frac{1}{\Delta J_i}\varepsilon^i\left(t\right) + \frac{\tau_i}{\Delta J_i}\dot{\varepsilon}^i(t) \qquad (3)$$

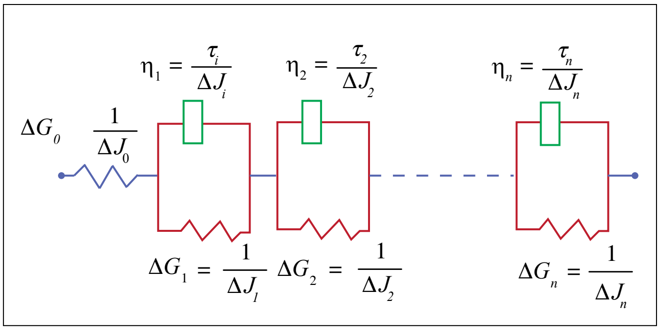

Figure 1—Generalized Kelvin model.

where:

τ_i is the retardation time;

i is the index of the block in the generalized Kelvin model;

and n is the number of blocks in the model:

$$\varepsilon\left(t\right) = \sigma\left(t\right)\sum_{i=0}^{n}\Delta J_i\left(\frac{\Delta t}{\Delta t + \tau_i}\right) + \sum_{i=0}^{n}\varepsilon^i\left(t - dt\right)\left(\frac{\tau_i}{\Delta t + \tau_i}\right) \qquad (4)$$

With this relationship, the viscoelastic displacement $u(t)$ is then deduced:

$$u\left(t\right) = l.\sigma\left(t\right)\sum_{i=0}^{n}\Delta J_i\left(\frac{dt}{dt + \tau_i}\right) + l.\sum_{i=0}^{n}u^i\left(t-dt\right)\left(\frac{\tau_i}{dt + \tau_i}\right) \qquad (5)$$

l is the length of the polyamide 6.6 specimen (small displacement assumption).

The relationship in Equation 5 is used to solve the load-sharing problem, but first it is necessary to determine the viscoelastic properties ΔJ_i and τ_i. Initial DMA tests reveal the evolution of the complex elastic compliance with the master curve; in a second test, a phenomenological model provides the numerical values of viscoelastic properties.

Experimental Characterization of Mechanical Properties

DMA tests were carried out with a spectrometer developed in the MATEIS laboratory (at the University of Lyon). This dynamic test enables determination of the evolution of the complex, elastic modulus or the complex elastic compliance function with the time or temperature. The tests were carried out in both dry and humid environments at 50% relative humidity.

Results and Viscoelasticity Modeling

For polymer material, the time/temperature superposition principle can be applied. With this principle—and the spectrometer tests—it is possible to build at a given reference temperature the storage-compliance curve $J'(i\omega,, T_{ref})$ or the loss-compliance curve $J''(i\omega, T_{ref})$ over a very wide frequency range. This "master curve" is obtained from the shift of experimental DMA curves obtained at different temperatures.

In order to determine the distribution of the retardation

continued

time τ_i, the numerical master curves $J'(i\omega\ T_{ref})$ are necessary. It is determined by using a phenomenological model as a numerical fit of the master curve. To do so, the bi-parabolic model developed by Decroix et al. is used (Ref. 10):

$$J^*\left(i\omega, T_{ref}\right) = \frac{1 + \delta\ \left(i\omega\tau'\right)^{-\chi} + \left(i\omega\tau'\right)^{-\chi'}}{\dfrac{1}{J_u} - \dfrac{1}{J_r}} + \frac{1}{J_r} \tag{6}$$

To obtain the time spectrum, discretization by pulsation of the numerical master curve $J_i'(i\omega, T_{ref})$ is needed. In this study, to account for the large relaxation time spectrum of the polyamide 6.6, it is necessary to use 19 elements of Kelvin-Voigt (*German physicist Woldemar Voigt*) in the Kelvin-generalized model. The distribution of retardation time $\tau_i\ (T_{ref})$ is deduced from pulsation ω_i at the maximum of $J_i''(i\omega, T_{ref})$, i.e.—in the middle of the frequency segment. The retardation time is deduced with the relation:

$$\tau_i = \frac{1}{\omega_i} \tag{7}$$

Figure 2 shows the experimental data and those issued from the generalized Kelvin model in a dry environment and 50% relative humidity.

Load-Sharing Model

The method developed by LaMCoS to model the instantaneous load-sharing is based on a unique process used for all types of gears made with steel or steel/polymer materials. This procedure has been used to model the load-sharing for cylindrical gears (Ref. 1); face gears (Ref. 2); spiral bevel gears (Ref. 3); worm gears (Ref. 4); and pinion racks (Ref. 5). This method is divided in three parts:

1. Simulation of manufacturing to obtain the tooth profile of the gear
2. Unloaded kinematics simulation to determine the potential contact zones
3. Computation of load-sharing between all teeth in contact

The relationship (Eq. 5) adapted for semi-crystalline materials has been integrated in the third step. This method yields results for transmission error, load-sharing and instantaneous pressure.

With a steel gear, the meshing used to solve the load-sharing is limited to the contact zone; indeed, this meshing occurs around the contact line. But contrary to steel gears, with polymer gears it is necessary to know the history of the gear and pinion displacements. Consequently, the meshing developed for the polymer gears is different from that of steel gears; it is larger—in tangent with the contact plane—and covers the entire tooth surface. Thus for a kinematics position it is possible to save the displacement of the entire profile of the pinion and gear in computing the following kinematics position.

In order to show some numerical examples for a spur gear made in polyamide 6.6 material, a standard geometry was used in this study. Figure 3 shows the tooth numbering used in the load-sharing model and Table 1 presents the gear data.

Equation of compatibility of displacement. Determination of tooth load-sharing is, above all, a multi-contact problem. The load-sharing problem is addressed by solving the equations of displacement compatibility (8–9) for every point k and driving torque (Eq. 10).

Inside the contact zone:

$$p\left(M_k\right) \geq 0 \ \text{ and } \ e\left(M_k\right) = \delta\left(M_k\right) + u\left(M_k\right) - \alpha = 0 \tag{8}$$

Outside the contact zone:

$$p\left(M_k\right) = 0 \ \text{ and } \ e\left(M_k\right) = \delta\left(M_k\right) + u\left(M_k\right) - \alpha \geq 0 \tag{9}$$

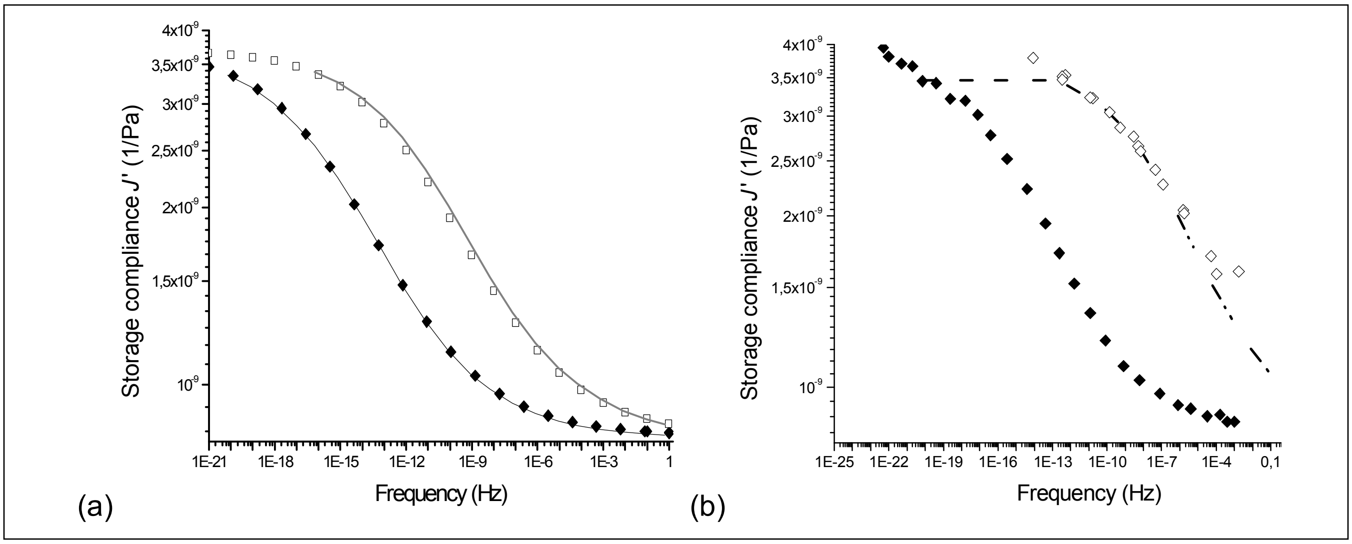

Figure 2—Master curves of storage compliance and fitting with model: a: (♦) dry test at T_{ref} = 0°C; (□) dry test at T_{ref} = 30°C; (–) dry model at T_{ref} = 0°C; (–) dry model at T = 30°C. b: (♦) dry test at T_{ref} = 0°C; (□) humid test (50% RH) at T_{ref} = 0°C; (--) humid model (50% RH) at T_{ref} = 0°C.

$$C_{motor} = \sum_{k=1}^{K} \left(p_k s_k \overrightarrow{n_k} \wedge \overrightarrow{M_k} \right) \tag{10}$$

K = number of nodes of the meshing
$P(M_k)$ = contact pressure at point M_k
$e(M_k)$ = gap between the profiles of the gear and pinion at point M_k—after the loading
$\delta(M_k)$ = gap between the profiles of the gear and pinion at point M_k—before the loading
$u(M_k)$ = displacement at point M_k
α = global body adjustment

The influence coefficient. In order to solve the load-sharing problem, it is necessary to compute the displacement u_k depending on pressure p_k. It is possible to indentify the relationship (Eq. 11) between displacement and pressure with use of the influence coefficients C_{kj}. There are two types of influence coefficients—the bulk-influence coefficients C^v_{kj} computed by finite element method, and the contact-influence coefficients C^s_{kj} computed by Boussinesq theory (*Ed.'s note: Joseph Valentin Boussinesq, nineteenth century French mathematician and physicist who made significant contributions to the theory of hydrodynamics, vibration, light and heat*).

$$u_k = \sum_{j=1}^{K} \text{ with } C_{kj} = C^v_{kj} + C^S_{kj} \tag{11}$$

However, the relationship in Equation 11 is adapted for steel gears; in the case of polymer gears, the geometrical-influence coefficient is used. They are defined by:

$$C_{kj} = J_{mat} C^*_{kj} \tag{12}$$

Viscoelastic displacement on meshing. In order to determine the nodes' displacement in the meshing, the displacement $u_k(t)$ is determined by the link between the relationships in Equations 5, 11 and 12.

$$u_k(t) = \sum_{i=1}^{n} u^i_k(t) \text{ with } u^i_k(t) = \sum_{j=1}^{K} C^*_{kj}\, p_j(t)\, \Delta J_l \left(\frac{dt}{dt+\tau_i} \right) + u^i_k(t-dt)\left(\frac{\tau_i}{\tau_i + dt} \right) \tag{13}$$

This system of equations, which includes the relationships in Equations 8–10, is used to calculate the load-sharing. This is done by using a fixed-point algorithm; it is also necessary to create a history of the displacements. To obtain this history, the displacement and the load-sharing are calculated for two teeth situated just before the tooth comes into contact.

Numerical results. Numerical examples for polyamide 6.6 spur gears are presented here; the gear data of the studied gears are presented in Table 1. Figure 4a shows the simulated load-sharing and Figure 4b shows the transmission error simulated for polymer gears at 25°C, 50% relative humidity, 300 rpm and 10 Nm. Figure 3 presents the tooth-numbering used for the simulated load-sharing.

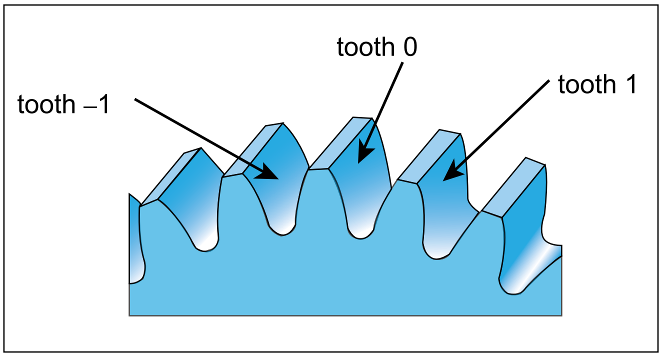

Figure 3—Tooth numbering.

Table 1—Gear Data

	Pinion	Gear
Module (mm)	3	3
Pressure angle (°)	20	20
Tooth width (mm)	20	20
Number of teeth	32	41

Figure 4a shows that the simulated load-sharing has a correct shape. With concurrent geometry simulation, Tooth –1 is unloaded and Tooth 1 is loaded gradually; Tooth 0—the central tooth—remains constant. Finally, for this gear geometry with material having a low elastic modulus and an important strain, there are always two teeth in contact.

The simulated transmission error shows that, at this temperature and in this relative humidity, the material behaves like a rubber material. The retardation time is brief—compared with the time scale of the rotation—and the apparent compliance is therefore high, leading to excessively high transmission error.

Experimental Measurements

Testing device. The unique characteristics of the LaMCoS bench are the instantaneous measure of the thermal behavior by an infrared camera, and transmission error. The gear data presented in Table 1 are used for this bench; Figure 5 shows the scheme of the test bench.

Transmission error measurements. The angular positions of pinion and gear are captured with optical encoders clamped directly on the rotating shaft, which is very useful for measuring transmission error because the encoders are now close to the gears. The principle of this measurement (Ref. 11) is based on counting pulses delivered by a timer at very high frequency (80 MHz) between two rising edges of the signal delivered by the optical encoders. This time-counting method must be carried out simultaneously on the two signals with the same reference; i.e., the same timer and counter. The time evolution of the pinion and gear angular positions is then defined with a sampling rate provided by the number of pulses on each encoder.

continued

The angular sampling method performs the calculation at the rising edge on the pinion signal and gear signal. The transmission error can be given as an angular displacement on either the pinion or gear shaft. With this method the relationship of the transmission error ε(*t*) as an angular displacement on the gear shaft is used:

$$\varepsilon(t) = \theta_2(t) - \frac{Z_1}{Z_2}\theta_1(t) \tag{14}$$

The test temperature is 25°C and relative humidity 50%. Figure 6 presents the comparison between transmission error measured and simulated at 25°C, 50% relative humidity, 300 rpm and 10 Nm. The simulation includes the assembling parameters as measured before the test; this transmission error is presented during the meshing of one tooth of the gear (8.57°).

This comparison is a good fit between the experimental

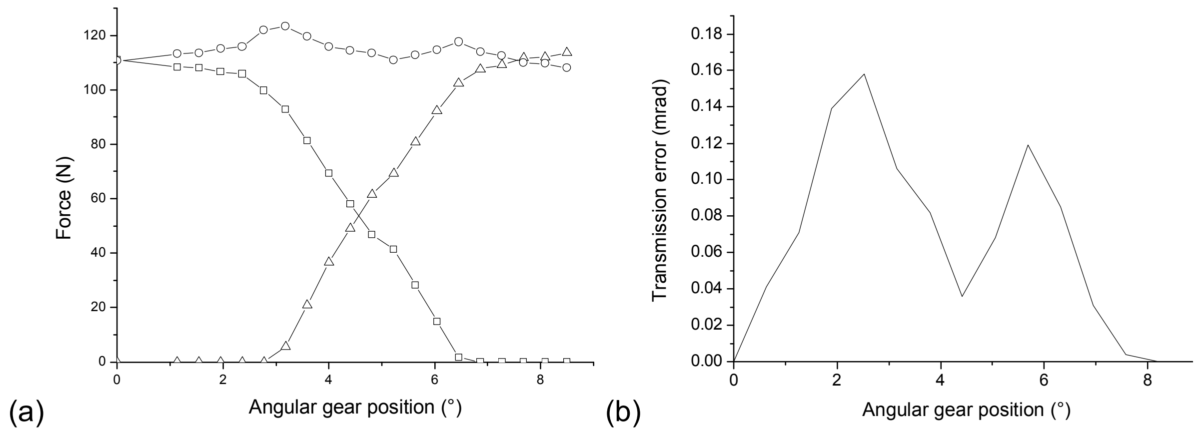

Figure 4—a: Load-sharing model at 25°C, 50% relative humidity, 300 rpm and 10 Nm; (□) Tooth -1; (o) Tooth 0; (Δ) Tooth 1. b: Transmission error at 25°C, 50% relative humidity, 300 rpm and 10 Nm.

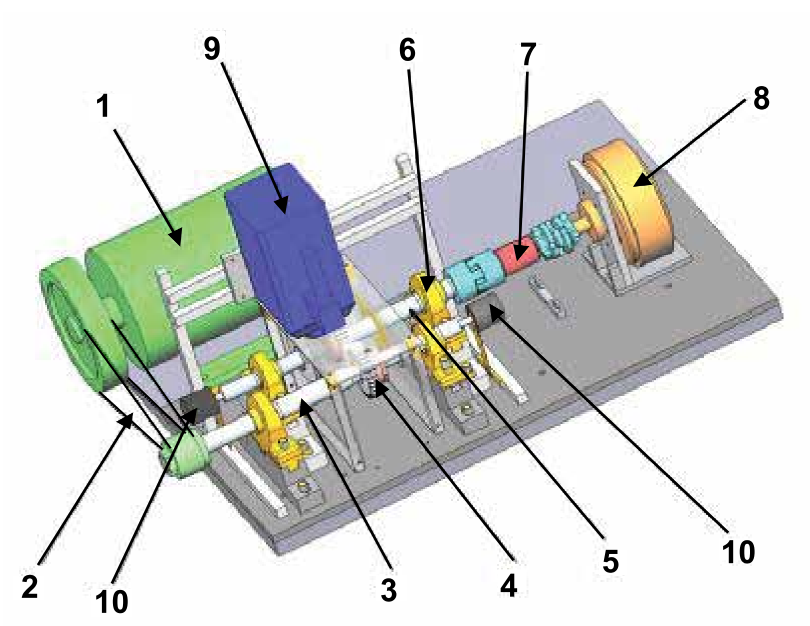

Figure 5—Test bench scheme, showing motor (1), belt (2), rotation axis of pinion (3), gears (4), rotation axis of gear (5), bearings (6), torquemeter (7), break (8), infrared camera (9) and optical encoders (10).

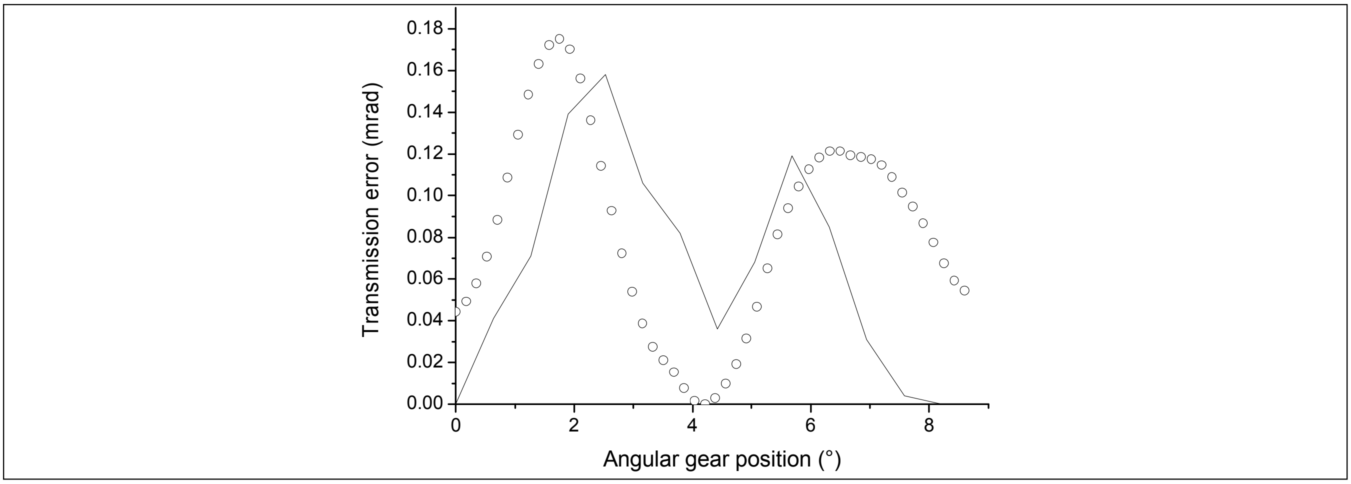

Figure 6—Comparison of measured and simulated transmission error at 25°C, 50% relative humidity, 300 rpm and 10 Nm; (o) = transmission error measured; (–) = simulated transmission error.

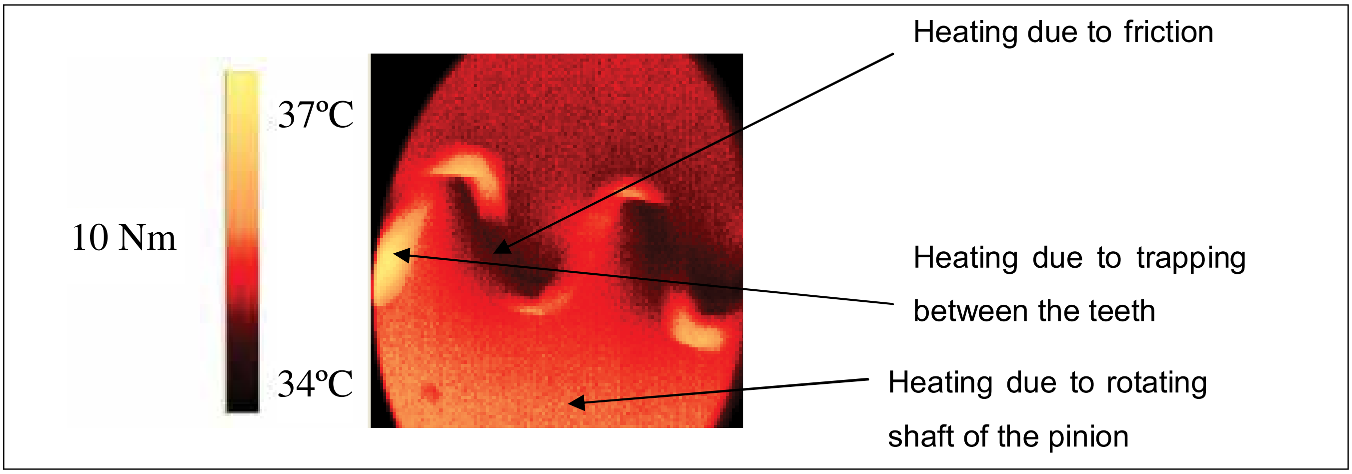

Figure 7—Measurements by infrared camera at 300 rpm and 10 Nm.

and numerical curves. Also, this figure shows that the simulated transmission error has the same shape and amplitude as that of the experimental transmission error.

Thermal measurements. In order to measure the thermal behavior of a polyamide 6.6 gear, an infrared camera was used. Figure 5 shows that the infrared camera (Eq. 9) is mounted on a support close to the gears. The optical encoder (Eq. 10) can trigger the camera at every turn of the pinion; however, the camera was set to record only when the same pair of teeth was in contact.

Thermal measurements are made on the profile of the teeth; but in order to do this, a polished mirror inclined at 45° was used, due to the vertical positioning of the camera; the polished mirror was aluminum-treated to facilitate the transfer of infrared thermal radiation. This solution enabled reflection of the image near the meshing to the camera—thus making it possible to measure the temperature of the gear. Figure 7 shows the results of the stabilized thermal measurements at 300 rpm and 10 Nm. These tests were made for 10 hours at a temperature of 25°C and 50% relative humidity.

The results show the different sources of heat generation with the friction between the teeth, the bearings with the shaft, and the trapping of air between the teeth. The temperature difference between the beginning and end of the test is 12.8°C. For the moment, the quasi-static load-sharing model does not take into account the heating during operation. However, Figure 2 shows that polymer gears are very sensitive to this temperature. The thermal results show that the quasi-static load-sharing model can be improved with the integration of a thermal model; i.e., one that accounts for the heating in the bulk and the contact during operation.

Conclusion

This study presents a fast and efficient method for studying the mechanical behavior of polyamide 6.6 spur gears. The viscoelastic properties are modeled with the generalized Kelvin model, which addresses the speed, temperature and humidity. With the viscoelastic displacement and the method of influence coefficients calculated on the entire surface of the tooth, it is therefore possible to overcome the load-sharing problem.

Also, this study showed an original, experimental test bench developed by LaMCoS. These experiments made possible the measurement of transmission error and thermal behavior of polyamide 6.6 gears. The measure of the transmission error shows a correct correlation between simulation and measurement. In addition, the simulation includes the

continued

precise tooth profile and parameters—assembling, temperature and speed. With thermal measurement it is possible to record the evolution and repartition of the meshing temperature function and determine the sources of heat generation. The next steps of the study will focus on the improvement of the quasi-static model via the thermal model.

References

1. Guingand, M., J.P. De Vaujany and Y. Icard. "Fast 3-D Quasi-Static Analysis of Helical Gears Using the Finite Prism Method," *Journal of Mechanical Design*, ASME, 6 (126) 2004, 1082–8.

2. Guingand, M., J.P. De Vaujany and Y. Icard. "Analysis and Optimization of the Loaded Meshing of Face Gears," *Journal of Mechanical Design*, ASME, 1 (127), 2005, 135–43.

3. Vaujany, J.P., M. Guingand, D. Remond and Y. Icard. "Numerical and Experimental Study of the Loaded Transmission Error of a Spiral Bevel Gear," *Journal of Mechanical Design*, SME, 2 (129), 2007, 129–35.

4. Hiltcher, Y., M. Guingand and J.P. De Vaujany. "Load-Sharing of a Worm Gear with a Plastic Wheel," *Journal of Mechanical Design*, ASME, 1 (129), 2007, 23–30.

5. De Vaujany, J.P. and M. Guingand. "Geometry, Kinematics and Load-Sharing of Pinion Rack Gear with Variable Ratio," *JSME International Conference on Motion and Power Transmissions*, Japan, May 13–15, 2009.

6. Haudin, J.M. "Structure and Morphology of Semi-Crystalline Polymers: Introduction to Mechanics of Polymers;" Ecole des Mines de Nancy, C. G'Sell and J.M. Haudin, 1995.

7.Lemaitre, J. and J.L. Chaboche. *The Mechanics of Solid Materials*, 2nd Ed. (French), 2004.

8.Scaffaro, R, N. Tzankova Dintcheva and F.P. La Mantia. "New Equipment to Measure the Combined Effects of Humidity, Temperature, Mechanical Stress and UV Exposure on the Creep Behavior of Polymers," *Polymer Testing*, Volume 27, Issue 1, February, 2008, pp. 49–54.

9. Ferry, J.D. *Viscoelastic Properties of Polymers*, 3rd Ed., John Wiley, 1980.

10. Decroix, J.Y., A. Piloz, A. Douillard, J.F. May and G. Valet. "Mathematical Model for Viscoelastic Behavior of Polyolefin: Application to Polyolefin Blends and Hexane-1-Propene Co-Polymers," *European Polymer Journal*, No. 11, 1975, 625–30.

11. Rémond, D. "Practical Performances of High-Speed Measurement of Gear Transmission Error or Torsional Vibration with Optical Encoders," *Journal of Measurement Science and Technology*, Volume 9, No. 3, 1990, pp. 347–53.

Jean-Pierre de Vaujany *is an associate professor (1997 to present) at the National Institute of Applied Sciences, INSA of Lyon/LaMCoS Laboratory, where he teaches mechanical design and CADD. De Vaujany also serves as director of the university's International Section Amerinsa (founded in 2000, coursework preparing graduate students for the international requirements that are essential in the engineering profession today).*

Michele Guingand *is a senior associate professor (1991 to present) at the National Institute of Applied Sciences, INSA of Lyon/LaMCoS Laboratory, where she teaches courses in gear design, CADD and product lifecycle management.*

Dr. Eric Letzelter *received his masters degree at the University of Strasbourg in 2007, specializing in mechanical and materials engineering. From 2007–2010 Letzelter taught mechanical engineering development at INSA Lyon before receiving his Ph.D. in 2011 at the Contact and Structural Mechanics Laboratory, LaMCoS of the INSA Lyon; his thesis: "The Mechanical Behavior Model of Polymer Cylindrical Gears." Letzelter is currently an engineer in the automotive industry.*